



Dynamic rolling force modeling of cold rolling strip based on mixed lubrication friction

Shuang Liu¹ · Huifeng Lu¹ · Dingxuan Zhao² · Runan Huang¹ · Jialei Jiang¹

Received: 7 October 2019 / Accepted: 30 March 2020 / Published online: 14 May 2020
© Springer-Verlag London Ltd., part of Springer Nature 2020

Abstract

The dynamic rolling force model in the coexistence regime of boundary lubrication friction and hydrodynamic lubrication friction was established in this paper, mainly aiming at the common mixed lubrication friction state in the actual rolling process, while the research of rolling mixed lubrication is relatively few. Combining Karman differential equation of unit pressure with Celikoff equation, a linearized differential equation of unit pressure was obtained. The expression of total friction stress under mixed lubrication state was given according to the oil film thickness at any position in the working area and the surface real contact area ratio. It is characterized by the consideration of the mixed lubrication friction state of the coexistence of boundary lubrication and hydrodynamic lubrication, which is applicable to the whole deformation zone and the general rolling mixed lubrication friction regime. The expressions of the unit normal pressure in the front-slip zone and the backward slip zone were obtained by considering the boundary conditions at the entry and exit cross sections. The dynamic rolling force model of cold rolling strip was established by numerical integral calculation. It is based on the above expression of total friction stress; therefore, this dynamic rolling force model is more universal, the prediction accuracy is higher, and it is closer to the actual industrial production. Based on the dynamic rolling force model, the effects of friction coefficient, reduction ratio, shear strength, and roll flattening on the unit normal pressure along the contact arc and the rolling force was also analyzed in this paper. Verification with actual industrial production data showed that the prediction model of rolling force had high precision, and it could provide guidance for calibration of rolling mill equipment and parameter optimization of production technology.

Keywords Rolling force · Mixed lubrication · Cold rolling · Friction stress

Nomenclature

A surface real contact area ratio
 B width of rolled piece
 C_0 roll flattening coefficient
 D diameter of work roll
 E modulus of elasticity of roll

H rolled piece inlet thickness
 h rolled piece outlet thickness
 Δh rolling reduction
 h_x oil film thickness at any position in the working area
 h_m the clearance between two contact surfaces or the nominal oil film thickness
 h_0 inlet oil film thickness
 K resistance of deformation
 k shear strength of the material
 K_1, K_2 friction characteristic coefficient
 l contact arc length
 p_x unit normal pressure
 p^- unit normal pressure in the backward slip area
 p^+ unit normal pressure in the front-slip area
 P rolling force
 q_h post-tension stress of rolled piece

✉ Dingxuan Zhao
zdx-yw@ysu.edu.cn

¹ School of Electrical Engineering, Yanshan University, Qinhuangdao 066000, China

² School of Mechanical Engineering, Yanshan University, Qinhuangdao 066000, China

q_H	front-tension stress of rolled piece
R_q	root-mean-square roughness
R_{q1}	roll surface roughness
R_{q2}	rolled piece surface roughness
R	radius of work roll
R'	roll radius after flattening
s_h	front-slip value
$u(x)$	rolled piece speed
u_1	rolled piece inlet velocity
u_2	exit speed of rolled piece
\bar{u}_1	average surface velocity
v	roll surface linear velocity
ν_r	Poisson ratio of roll
x_n	horizontal coordinates of neutral plane
α	angle of inlet
γ_1	pressure coefficient of viscosity
λ	coefficient of extension
ε_0	the viscosity of lubricating oil
ε	reduction ratio
τ	total friction stress
τ_a	boundary lubrication friction stress
τ_b	hydrodynamic lubrication friction stress
μ	friction coefficient
μ_0	viscosity at atmospheric pressure
σ	yield stress of rolled piece material

1 Introduction

Rolling is usually referred to as the process in which steels are transferred between two rollers of the mill so as to reduce the thickness [1]. Rolling is one of the most basic methods to produce the board strip material [2]. The common rolling state is divided into cold rolling and hot rolling [3]. Numerous investigations have been carried out to analyze the cold and hot rolling process [4], most of the cold rolling process needs to be lubricated, while the hot rolling process involves high temperatures and pressures [5]. In recent years, with the rapid development of the science and technology, the demand for the board strip material is growing fast in all professions and trades, and the quality requirements are also becoming higher and higher [6]. The accurate prediction model of rolling force is of great significance to ensure the stable operation of rolling process, to control the profile and thickness of the board strip material and to improve the quality of products [7–9]. Therefore the rolling force modeling of cold rolling and hot rolling has always been one of the hot spots in the research of rolling field. Most of the current rolling force models are derived from the basic theory of Kanman and Orowan [10, 11], and these models have simplified the hypothetical conditions to some extent when solving complex differential equations of unit pressure [12]. Generally speaking, lubrication in rolling process helps to reduce roll strip friction and roll wear and

plays an important role in improving the surface quality of steel products [13]. At the same time, the research of rolling lubrication is also deepening [14, 15]. The roll gap after the addition of the lubricant is usually under the mixed lubrication friction state of the coexistence of the boundary lubrication friction and the hydrodynamic lubrication friction [16]. Some steel materials related to surface treatment need to be manufactured under the condition of mixed lubrication friction, so that the products can obtain better surface morphology [17]. However, the research on rolling mixed lubrication is relatively few, and the operation mechanism of rolling technology process under the mixed lubrication friction regime is not explicit. Some studies are more concerned with dry friction or boundary lubricating friction [18, 19], while others are limited to hydrodynamic lubrication friction [20, 21], which is clearly not sufficient to reflect the complex situations of the roll gap. Therefore, it is of great significance to study the rolling process state and process parameter setting under mixed lubrication friction. The analysis of the process parameters such as friction lubrication state and the changes of rolling pass thickness in rolling process is the important content of rolling force modeling [22, 23].

So far, a great deal of research has been done on mechanical modeling, lubrication friction, and other problems in the rolling process. Lin [24] integrating a neural network and an incremental updated the Lagrangian elasto-plastic finite-element method to predict the rolling force and the maximum surface error during the rolling process, then established a model for the rolling variables through input the results of them to a neural network. This work achieved a satisfactory result and was a new and feasible approach which could be used for control of the rolling process for materials. Wu et al. [25] calculated the shear stress of lubricant by using the shear term of lubricant and the pressure driving term and presented a simple robust method for solving the flow field and solid field. This method gave a new understanding of the effect of rolling speed and pressure coefficient on hydrodynamic pressure and lubrication film thickness. By using the extended Bernoulli theorem of pressure and velocity on arbitrary streamline, Alexandrov et al. [26] extended the flow theory of isotropic rigid ideal plastic materials to the general orthotropic materials which accord with the maximum plastic dissipation principle. Using the generalized Bernoulli theorem of pressure and velocity on arbitrary streamlines presents a simple relation between the process parameters and constitutive parameters in the ductile fracture criterion, and this relation is applicable to the rapid design of metal forming processes. Stratmann et al. [27] had studied the influence of lubrication condition and sliding roll ratio on the formation of friction film in a bearing test stand. The experimental results showed that higher SRR value would hinder the growth of friction film and accelerate the growth of the tribofilm after the initial film formation. The growth of tribological film at higher rotation speed was

supported by higher friction energy input. This research will encourage the development of predicting antiwear for rolling bearings. Cao et al. [28] obtained the internal deformation power and the friction power by using angular bisector yield criterion and Pavlov projection principle in the vertical rolling the first time and the simpler analytical solutions of total power and separating rolling force by using an energy method. Compared with the online measurement of hot rolling strip, the relative error of rolling force is less than 8.29%, which is of great significance to the width control of the vertical rolling of the hot rolling strip. Moreover, the formula forms of the internal deformation power, the friction power, and the shear power are greatly simplified and improved.

In the existing research, Chen et al. [29], based on the comprehensive consideration of the sliding and adhesion friction on the contact arc, are giving an improved Karman equation for hot rolling strip and establishing a new expression for rolling force. The distribution of rolling force along the contact arc was obtained by Runge-Kutta method. The actual industrial application verification showed that the proposed new model enhances the setting precision of rolling force and can be applied to online control of hot rolling strip. However, this article still treated the lubrication state respectively in the sliding zone and the adhesive zone and did not unify together the two lubrication friction states. Wu et al. [30] proposed a new multi-scale method for the study of interfacial pressure and friction in three-dimensional model of cold rolling strip. The main innovation is to combine the lubrication effect with the surface asperity deformation by using the equivalent interfacial layer. The proposed method could be used to obtain the deformation situation of the micro roller strip interface, deal with the dynamic lubrication state from hydrodynamic lubrication to mixed lubrication to boundary lubrication, and predict accurately the experimental results and was suitable for other contact sliding processes under complex lubrication regimes. However, this article only studied the interface pressure under complex mixed lubrication conditions, but did not involve the prediction modeling of rolling force. Using the global weighting method, Zhang et al. [31] successfully established a new 3D velocity field for steel plate rolling and derived out in detail the specific linear plastic power of the MY yield criterion. The rolling force, torque, and the stress influence factors were obtained by minimizing the power functional. Compared with the experimental results, the maximum error rate between them was less than 15.5%. However, the prediction accuracy of the rolling force model obtained in this paper was not good enough, which was of little significance to the application of actual industrial production. Sun [32] analyzed the fundamental formulae of cold rolling strip and pointed out some important characteristics of cold rolled strip. On the premise of dry friction theory, the Karman differential equation of unit pressure and the Celikoff formula were solved and analyzed in

detail. However, the impact of boundary lubrication or hydrodynamic lubrication on rolling force was not comprehensive considered in this paper.

In the actual rolling process, because of the rupture of the lubricating oil film or the existing of roughness, there is often a direct contact area between the surface of roller and rolling piece, which can be known on the basis of similar imprints on the surface of roller and rolling piece, the roll gap is usually under the mixed lubrication regime of the coexistence of boundary lubrication friction and hydrodynamic lubrication friction. However, the operation mechanism of rolling technology process under the mixed lubrication friction regime is still not explicit. Therefore, it is of great significance to study the rolling process state and process parameter setting under mixed lubrication friction. In addition, at present, a large number of rolling force models often adopt some hypothetical conditions, and rarely involve mixed lubrication friction, which makes them simple structure, poor accuracy, and cannot be competent for the setting of rolling process site model parameters. Therefore, it has very important significance to create a rolling force model with wide range of application, considering mixed lubrication friction and high precision.

Targeting these existing problems, firstly, the unit pressure differential equation after linearization and the expressions of total friction stress under the mixed lubrication regime was obtained, based on the Karman unit pressure differential equation and the surface real contact area ratio. The total friction stress takes into account the mixed lubrication friction of the coexistence of boundary lubrication and hydrodynamic lubrication, and it is applicable to the whole deformation zone and the general rolling mixed lubrication friction regime. Furthermore, considering the boundary conditions at entrance and exit cross sections, the expression of unit normal pressure in front and backward slip area was given and we also established the dynamic rolling force model of cold rolling strip under the mixed lubrication friction state. The friction stress of the rolling force model was partly the boundary lubrication friction stress generated by the rough contact surface, and the other part was the hydrodynamic lubrication friction stress caused by the lubricating oil in the groove of the contact surface; therefore, it is more universal, the prediction accuracy is higher, and it is closer to the actual industrial production. Finally, based on the dynamic rolling force model, the effects of friction coefficient, reduction ratio, shear strength, and roll flattening on the distribution of unit normal pressure along the contact arc and the rolling force were also analyzed. The verification of actual industrial production data showed that the model could be used for online prediction of rolling force in the process of cold rolling strip production.

2 The Celikoff solution of Karman differential equation of unit pressure

The general form of Karman unit pressure differential equation [33] is:

$$\frac{dp_x}{dx} - \frac{K}{y} \frac{dy}{dx} \pm \frac{\tau}{y} = 0 \tag{1}$$

Celikoff regards the contact arc as a string, as shown in Fig. 1, taking the end point of the deformation zone as a vertical line is the y axis and the central axis of the rolled piece as the x axis.

Then, the coordinate of point A is $(l, \frac{H}{2})$, B is $(0, \frac{h}{2})$

and the straight line equation through A and B is

$$y = \frac{\Delta h}{2l}x + \frac{h}{2} \tag{2}$$

After differential

$$dy = \frac{\Delta h}{2l}dx \text{ or } dx = \frac{2l}{\Delta h}dy \tag{3}$$

By using the Celikoff solution, we can obtain

$$\frac{dp_x}{dx} - \frac{K}{y} \frac{\Delta h}{2l} \pm \frac{\tau}{y} = 0 \tag{4}$$

Equation (4) is the unit pressure differential equation after linearization. This linearization means that the contact arc is treated as a straight line, that is, the strings of the contact arc is

used instead of the arc. The plus sign indicates the backward slip area, and the minus sign indicates the front-slip area.

3 Total friction stress of dynamic roll gap under mixed lubrication

3.1 Typical expression of total friction stress

With the gradual increase of rolling speed, the thickness of oil film of the roll gap becomes larger. However, due to the oil film rupture or the existence of surface roughness, the rolling process is usually under the mixed lubrication friction state of the coexistence of the sliding friction generated by the direct contact between the roller and the rolled piece and the hydrodynamic lubrication friction produced by the lubricating oil film. In this state, the typical expression of the total friction stress is:

$$\tau = A\tau_a + (1-A)\tau_b \tag{5}$$

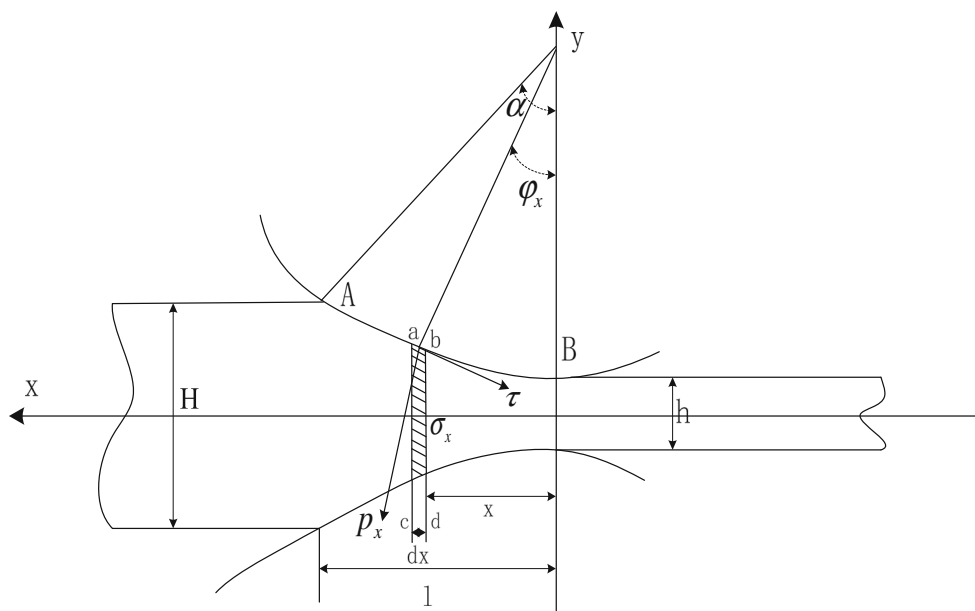
It is assumed that τ_a generated by the rough contact surface can be calculated from the adhesive friction theory: $\tau_a = k \cdot \tau_b$ produced by the lubricating oil film can be calculated by the following equation:

$$\tau_b = \varepsilon_0 \frac{(u(x)-v)}{h_x} \tag{6}$$

3.2 Surface real contact area ratio

A part of the mixed lubrication friction state is the sliding friction generated by the direct contact between the rough

Fig. 1 Schematic diagram of force analysis of differential element body



peaks of the surface between the roll gap. It is generally assumed that the height distribution of surface roughness of the roll, and the rolled piece is Gauss distribution, so the surface real contact area ratio A can be estimated. Christensen proposed an approximation value to substitute the Gauss distribution [34], so the probability density function $f(z)$ of a certain height z is:

$$f(z) = \frac{35}{96R_q} \left[1 - \frac{1}{9} \left(\frac{z}{R_q} \right)^2 \right]^3 \quad |z| \leq 3R_q \tag{7}$$

$$f(z) = 0 \quad z > 3R_q$$

$$f(z) = 0 \quad z < -3R_q$$

where $R_q = \sqrt{R_{q1}^2 + R_{q2}^2}$.

Combined with Fig. 2, A can be obtained by integrating the probability density function

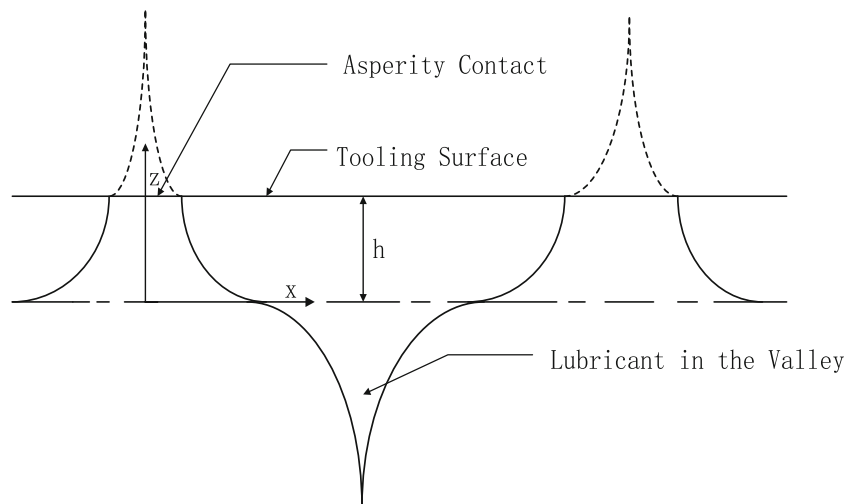
$$A = \int_{-h}^{\infty} f(z) dz = \int_{-h}^{3R_q} f(z) dz + \int_{3R_q}^{\infty} f(z) dz \tag{8}$$

As $z > 3R_q, f(z) = 0$, then: $\int_{3R_q}^{\infty} f(z) dz = 0$, so only the first half of the upper equation is left, and the calculation results are as follows:

$$A = \frac{1}{2} - \frac{1}{96} \left[\frac{35h_m}{R_q} - \frac{35}{9} \left(\frac{h_m}{R_q} \right)^3 + \frac{7}{27} \left(\frac{h_m}{R_q} \right)^5 - \frac{5}{729} \left(\frac{h_m}{R_q} \right)^7 \right] \tag{9}$$

where the value of h_m is 0.002(mm).

Fig. 2 Christensen’s contact diagram of surface roughness



3.3 Oil film thickness at any position in the working area and total friction stress

The other part of mixed lubrication friction state is the hydrodynamic lubrication friction generated by the lubricating oil film. h_x and h_0 must satisfy the flow rate continuity condition

$$h_x = \frac{v + u_1}{v + u(x)} h_0 \tag{10}$$

According to the principle of the equal of flow rate of metal seconds: $u_1 = \frac{u_2}{\lambda}$, where $u_2 = v(1 + s_h)$, so $u_1 = \frac{v(1+s_h)}{\lambda}$, where $\lambda = 1.3$, s_h uses the following formula:

$$s_h = \frac{\Delta h}{4h} \left(1 - \frac{1}{2\mu} \sqrt{\frac{\Delta h}{R}} \right)^2 \tag{11}$$

$u(x)$ can be determined by the following equation

$$u(x) = u_1 \frac{H}{y(x)} \tag{12}$$

where $y(x)$ is the rolled piece thickness in the working area

$$y(x) = H(1-\varepsilon) + \frac{x^2}{R} \tag{13}$$

Eq. (13) is substituted in Eq. (12)

$$u(x) = u_1 \frac{H}{H(1-\varepsilon) + \frac{x^2}{R}} = \frac{RHu_1}{x^2 + RH(1-\varepsilon)} \tag{14}$$

where

$$u_1 = \frac{v}{\lambda} \left[1 + \frac{\Delta h}{4h} \left(1 - \frac{1}{2\mu} \sqrt{\frac{\Delta h}{R}} \right)^2 \right] \tag{15}$$

where μ can be approximately represented by Roberts’s formula according to ref [35]:

$$\mu = \sqrt{\frac{\Delta h}{D}} [0.5 + (K_1 - 0.5)e^{-K_2 v}] \tag{16}$$

where $K_1=3.61, K_2=0.001$.

In isothermal case, taking the effect of post-tension of rolled piece into account, the common calculation formula for h_0 according to ref [16] is as follows:

$$h_0 = \frac{6\gamma_1\mu_0\bar{u}_1}{\alpha(1-e^{-\gamma_1(\sigma-q_h)})} \tag{17}$$

where $\bar{u}_1 = \frac{u_1+v}{2}$.

In conclusion

$$h_x = \frac{v + u_1}{v + \frac{RHu_1}{x^2 + RH(1-\varepsilon)}} \cdot h_0 = \frac{(v + u_1)(x^2 + RH(1-\varepsilon))}{vx^2 + RH(u_1 + v(1-\varepsilon))} \cdot h_0 \tag{18}$$

The total friction stress under mixed lubrication is expressed as follows:

$$\begin{aligned} \tau &= A\tau_a + (1-A)\tau_b = Ak + (1-A)\varepsilon_0 \frac{(u(x)-v)}{h_x} \\ &= Ak + (1-A)\varepsilon_0 \frac{(HRu_1)^2 - (v(x^2 + HR(1-\varepsilon)))^2}{(v + u_1)(x^2 + HR(1-\varepsilon))^2 h_0} \end{aligned} \tag{19}$$

The total friction stress takes into account the mixed lubrication friction of the coexistence of boundary lubrication and hydrodynamic lubrication, and it is applicable to the whole deformation zone and the general rolling mixed lubrication friction regime.

4 Dynamic rolling force model of cold rolling strip

4.1 Differential equation of unit normal pressure in backward slip zone

$$\frac{dp_x}{dx} - \frac{K \Delta h}{y} \frac{1}{2l} + \frac{\tau}{y} = 0 \tag{20}$$

Using p^- instead of p_x , combine with (2) and multiplying both sides by dx , we can obtain

$$dp^- = \left(\frac{K \cdot \Delta h}{2l} - \tau \right) \frac{1}{\left(\frac{\Delta h}{2l} x + \frac{h}{2} \right)} dx \tag{21}$$

By integrating both sides of the upper equation

$$p^- = \frac{2l}{\Delta h} \left(\frac{K \cdot \Delta h}{2l} - \tau \right) \ln \left(\frac{\Delta h}{2l} x + \frac{h}{2} \right) + C_0 \tag{22}$$

According to the boundary condition, at the entrance cross section, as $x = l, p^- = K - q_H$, these two equations are substituted in the above equation

$$C_0 = K - q_H - \frac{2l}{\Delta h} \left(\frac{K \Delta h}{2l} - \tau \right) \ln \left(\frac{H}{2} \right) \tag{23}$$

To sum up, the equation of the unit normal pressure in the backward slip area is as follows:

$$p^- = \left(K - \frac{2l \cdot \tau}{\Delta h} \right) \ln \left(\frac{\Delta h}{Hl} x + \frac{h}{H} \right) + K - q_H \tag{24}$$

4.2 Differential equation of unit normal pressure in front-slip zone

$$\frac{dp_x}{dx} - \frac{K \Delta h}{y} \frac{1}{2l} - \frac{\tau}{y} = 0 \tag{25}$$

Using p^+ instead of p_x , similarly

$$p^+ = \frac{2l}{\Delta h} \left(\frac{K \cdot \Delta h}{2l} + \tau \right) \ln \left(\frac{\Delta h}{2l} x + \frac{h}{2} \right) + C_1 \tag{26}$$

According to the boundary conditions, at the exit cross section, as $x = 0, p^+ = K - q_h$, these two equations are substituted in the above equation

$$C_1 = K - q_h - \frac{2l}{\Delta h} \left(\frac{\Delta h \cdot K}{2l} + \tau \right) \ln \left(\frac{h}{2} \right) \tag{27}$$

To sum up, the equation of the unit normal pressure in the front-slip area is as follows:

$$p^+ = \left(K + \frac{2l}{\Delta h} \tau \right) \ln \left(\frac{\Delta h}{h \cdot l} x + 1 \right) + K - q_h \tag{28}$$

4.3 Dynamic rolling force model

The total rolling force in the deformation zone is:

$$P = B \times l \times \int_0^l p_x dx = B \times \int_0^l p_x dx = B \times \left(\int_{x_1}^{x_2} p^- dx + \int_{x_2}^{x_1} p^+ dx \right) \tag{29}$$

The differential equation of unit normal pressure in front and backward slip zone is substituted in the above equation

$$P = B \times \left\{ \int_{x_n}^l \left\{ \left(K - \frac{2l \cdot \tau}{\Delta h} \right) \ln \left(\frac{\Delta h}{Hl} x + \frac{h}{H} \right) + K - q_H \right\} dx + \int_0^{x_n} \left\{ \left(K + \frac{2l \cdot \tau}{\Delta h} \right) \ln \left(\frac{\Delta h}{hl} + 1 \right) + K - q_h \right\} dx \right\} \tag{30}$$

The total friction stress is substituted in the above equation, and the term which cannot be properly integrated is treated by Taylor series approximation to obtain

$$P = B \times \left\{ \int_{x_n}^l \left\{ \left(K - \frac{2l}{\Delta h} Ak + \frac{2l}{\Delta h} (1-A) \varepsilon_0 \frac{v^2}{(v + u_1) h_0} \right) \ln \left(\frac{\Delta h}{Hl} x + \frac{h}{H} \right) + K - q_H \right\} dx + \int_0^{x_n} \left\{ \left(K + \frac{2l}{\Delta h} Ak - \frac{2l}{\Delta h} (1-A) \varepsilon_0 \frac{v^2}{(v + u_1) h_0} \right) \ln \left(\frac{\Delta h}{hl} x + 1 \right) + K - q_h \right\} dx + \frac{2l}{\Delta h} \varepsilon_0 \frac{(HRu_1)^2}{(v + u_1) h_0} \left[\int_0^{x_n} \left\{ (1-A) \frac{\ln(cx + 1)}{(x^2 + HR(1-\varepsilon))^2} \right\} dx - \int_{x_n}^l \left\{ (1-A) \frac{\ln(ax + b)}{(x^2 + HR(1-\varepsilon))^2} \right\} dx \right] \right\} \tag{31}$$

where

$$\ln(ax + b) = \ln b + \frac{a}{b} x - \frac{a^2}{2b^2} x^2 + \frac{a^3}{3b^3} x^3 - \frac{a^4}{4b^4} x^4 + \frac{a^5}{5b^5} x^5 - \frac{a^6}{6b^6} x^6, a = \frac{\Delta h}{Hl}, b = \frac{h}{H},$$

$$\ln(cx + 1) = cx - \frac{c^2}{2} x^2 + \frac{c^3}{3} x^3 - \frac{c^4}{4} x^4 + \frac{c^5}{5} x^5 - \frac{c^6}{6} x^6, c = \frac{\Delta h}{hl}.$$

The following is the integration of the above equation

$$P = B \times \left\{ \left\{ N_1 x \ln \left(\frac{\Delta h}{H \cdot l} x + \frac{h}{H} \right) + \frac{N_1 hl}{\Delta h} \ln(\Delta h \cdot x + hl) + (K - N_1 - q_H) x \right\} \Big|_{x_n}^l + \left\{ N_2 x \ln \left(\frac{\Delta h}{h \cdot l} x + 1 \right) + \frac{N_2 hl}{\Delta h} \ln(\Delta h \cdot x + hl) + (K - N_2 - q_h) x \right\} \Big|_0^{x_n} + \frac{2l}{\Delta h} \cdot \varepsilon_0 \frac{(HRu_1)^2}{(v + u_1) \cdot h_0} \left\{ \ln \left(6x \sqrt{N_{10}} + N_9 + N_8 + N_6 + N_4 + N_3 \right) \times \left(\frac{a_3^3}{6} + N_5 + N_7 \right) - \frac{a_3^6 x^3}{18} + \ln \left(6x \sqrt{N_{10}} + N_9 + N_8 - N_6 - N_4 - N_3 \right) \cdot \left(\frac{a_3^3}{6} + N_5 - N_7 \right) + \frac{a_3^5 x^2}{10} - x \left(\frac{a_3^4}{4} - \frac{HRa_3^6(1-\varepsilon)}{3} \right) x \cdot \left(5H^2 R^2 a_3^6 \cdot (\varepsilon - 1)^2 + \frac{15HRa_3^4}{2} (\varepsilon - 1) + 15a_3^2 \right) - 6H^2 R^2 a_3^5 (\varepsilon - 1)^2 - 10HRa_3^3 (\varepsilon - 1) - 30a_3 \right\} \Big|_0^{x_n} + \frac{2l}{\Delta h} \cdot \varepsilon_0 \frac{(HRu_1)^2}{(v + u_1) \cdot h_0} \left\{ \ln(x \cdot N_{22} + N_{16} - N_{15} + N_{14}) \cdot \left(\frac{N_{11} + N_{18} - N_{12}}{N_{19}} - N_{17} + N_{13} \right) + \ln(x \cdot N_{22} - N_{16} + N_{15} - N_{14}) \cdot \left(\frac{N_{11} - N_{18} - N_{12}}{N_{19}} + N_{17} + N_{13} \right) - \left(\frac{a_1^4}{4a_2^4} - \frac{HRa_1^6(1-\varepsilon)}{3a_2^6} \right) x + \frac{a_1^5 x^2}{10a_2^5} - \frac{a_1^6 x^3}{18a_2^6} - \frac{30a_1 a_2^5 + 10HRa_1^3 a_2^3 (\varepsilon - 1) + 6H^2 R^2 a_1^5 a_2 (\varepsilon - 1)^2}{60a_2^6 (x^2 + HR - HR\varepsilon)} \right\} \Big|_0^{x_n} + \frac{5x \left(12a_2^6 \ln(a_2) + 2H^3 R^3 a_1^6 (1-\varepsilon)^3 - 3H^2 R^2 a_1^4 a_2^2 (1-\varepsilon)^2 + 6HRa_1^2 a_2^4 (1-\varepsilon) \right)}{(2HR(1-\varepsilon))(60a_2^6 (x^2 + HR - HR\varepsilon))} \Big|_{x_n}^l \right\} \tag{32}$$

Table 1 Data information of the steel coil

Coil number BN ZN	Steel grade ST.MK	Strip width <i>B</i> (mm)	Incoming material thickness <i>H</i> (mm)	Finished product thickness <i>h</i> (mm)	Work roll diameter <i>D</i> (mm)	Original deformation resistance <i>K</i> (MPa)
510202 981500	Q 195	1200	2.605	0.37	416	730

where,

$$\begin{aligned}
 N_1 &= K - \frac{2l}{\Delta h} Ak + \frac{2l}{\Delta h} \cdot (1-A) \cdot \varepsilon_0 \frac{v^2}{(v + u_1)h_0}, N_2 = K + \frac{2l}{\Delta h} Ak - \frac{2l}{\Delta h} (1-A) \cdot \varepsilon_0 \frac{v^2}{(v + u_1)h_0}, \\
 N_3 &= 10H^3R^3a_3^4(\varepsilon-1)^3, N_4 = 9H^2R^2a_3^2(\varepsilon-1)^2, N_5 = \frac{HRa_3^5(\varepsilon-1)}{5}, N_6 = 6HR(\varepsilon-1), \\
 N_7 &= \frac{a_3^2}{8\sqrt{N_{10}}} + \frac{3a_3^4\sqrt{N_{10}}}{16} + \frac{5a_3^6N_{10}^{1.5}}{24}, N_8 = 10a_3^4xN_{10}^{2.5}, N_9 = 9a_3^2xN_{10}^{1.5}, N_{10} = HR(\varepsilon-1), \\
 N_{11} &= \frac{H^3R^3a_1^3a_2^3}{6}, N_{12} = \frac{H^4R^4a_1^5a_2}{5}, N_{13} = \frac{HRa_1^5\varepsilon}{5a_2^5}, N_{14} = H^2R^2\varepsilon^2, N_{15} = 2H^2R^2\varepsilon, \\
 N_{16} &= H^2R^2, N_{17} = \frac{\frac{a_2^6 \ln(a_2) N_{22}}{4} - \varepsilon \left(\frac{N_{20}}{8} - N_{21} \right) + \frac{N_{20}}{16} - N_{21} + \frac{3H^2R^2a_1^4a_2^2\varepsilon^2N_{22}}{16}}{H^3R^3a_2^6(1-\varepsilon)^3}, \\
 N_{18} &= \frac{5H^3R^3a_1^6N_{22}}{24}, N_{19} = H^3R^3a_2^6, N_{20} = 3H^2R^2a_1^4a_2^2N_{22}, N_{21} = \frac{HRa_1^2a_2^4N_{22}}{8}, \\
 N_{22} &= \sqrt{H^3R^3(\varepsilon-1)^3}.
 \end{aligned}$$

If the total friction stress is assumed to be constant: $\tau = \mu \cdot K$, this equation is substituted in Eq. (30), and the original rolling force model is as follows:

$$\begin{aligned}
 P &= B \times \left\{ \int_{x_n}^l \left\{ \left(K - \frac{2l \cdot \mu K}{\Delta h} \right) \ln \left(\frac{\Delta h}{Hl} x + \frac{h}{H} \right) + K - q_H \right\} dx \right. \\
 &\quad \left. + \int_0^{x_n} \left\{ \left(K + \frac{2l \cdot \mu K}{\Delta h} \right) \ln \left(\frac{\Delta h}{hl} + 1 \right) + K - q_h \right\} dx \right\} \quad (33)
 \end{aligned}$$

Table 2 Comparison of the rolling production site data of each rolling pass and the calculation result of the improved model and the original model

Rolling pass no.	Inlet thickness <i>H</i> (mm)	Outlet thickness <i>h</i> (mm)	Post-tension stress <i>q_n</i> (MPa)	Reduction ratio ε (%)	Rolling speed (m/s)
1	2.605	1.755	134	32.6	3.9
2	1.755	1.117	133	36.4	6.2
3	1.117	0.74	141	33.8	9.4
4	0.74	0.493	143	33.4	14
5	0.493	0.37	56	24.9	18.4
Measured rolling force (kN)	Improved rolling force model (kN)	Original rolling force model (kN)	Improved prediction error (%)	Original prediction error (%)	
9212	10,160	15,227	10.3	66.3	
9771	9776	14,398	0.05	47.4	
8918	7755	10,321	-13.04	15.7	
7673	6649	8249	-13.34	7.5	
7095	6234	5269	-12.13	-25.7	

Equation (32) is the dynamic rolling force model of cold rolling strip based on mixed lubrication friction. Where the contact arc length $l = \sqrt{R \cdot \Delta h}$, the neutral point x_n can be obtained according to the equal of the unit normal pressure in the backward slip area and the front-slip area. Its characteristic lies in that the mixed lubrication friction state in which the coexistence of boundary lubrication friction and hydrodynamic lubrication friction is comprehensively considered. With the wide use of lubricant and the continuous improvement of rolling speed, the mixed lubrication friction state is becoming more and more common in the rolling process. Therefore, compared with the similar model, this dynamic rolling force model is more universal, the prediction accuracy is higher, and it is closer to the actual industrial production.

5 Verification of prediction accuracy and analysis

5.1 Verification of prediction accuracy

The data collected from the actual production site of the State Key Laboratory of Northeast University was adopted in this paper. Its material data, rolling parameters, and the comparison results are shown in Tables 1 and 2.

The deformation resistance in Table 1 can be calculated on the basis of ref [32], that is $K = 200.94 + (69673.55\varepsilon + 13475.18)^{0.5974}$. Improved rolling force model in Table 2 represents the dynamic rolling force model corresponding Eq. (32) and original rolling force model the Eq. (33). As shown in Table 1 and Table 2, the prediction error of the improved model is kept within $\pm 13.34\%$, which is highly accurate. The prediction error of the original model is only no. 3 and no. 4 set of data are quite ordinary, while the prediction error of no. 1 is 66.3% and the no. 2 is 47.4%, which is extremely disappointing. These results testify that the dynamic rolling force prediction model has high prediction accuracy and be able to better get close to the actual industrial production situation. Therefore, it can provide guidance for prediction of rolling force in the process of cold rolling strip production, the verification of the rolling mill equipment, and the parameter optimization of the production technology.

5.2 Impact of friction coefficient on unit normal pressure and rolling force

As shown in Fig. 3, the unit normal pressure increases with the increase of the friction coefficient, and it gets the maximum at the neutral point. As shown in Fig. 4, with the increase of friction coefficient, the rolling force is also increasing. When the friction coefficient exceeds 0.3, the increase of both unit normal pressure and rolling force is getting slower. This is

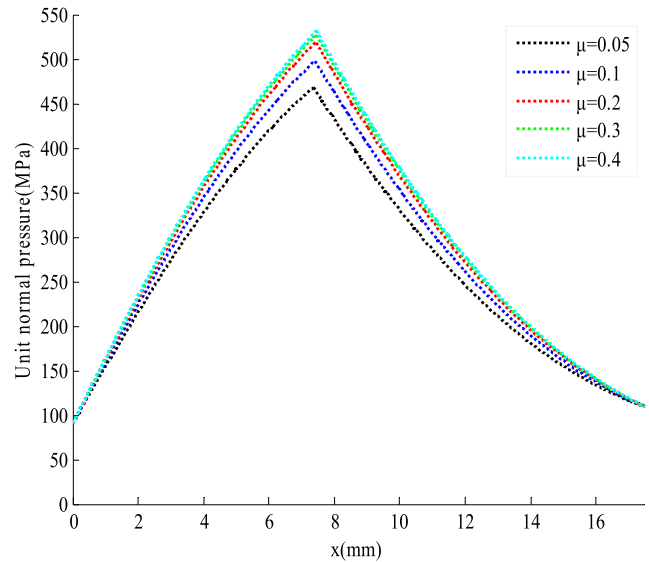


Fig. 3 Changes of unit normal pressure with friction coefficient

because with the increase of friction coefficient, the proportion of lubricating friction is becoming smaller, and the rolling state is closer to dry friction. When the friction coefficient increased from 0.05 to 0.2, the rolling force increased significantly by nearly 20%. Therefore, if appropriate measures can be taken to improve the lubrication friction state in the rolling process, the rolling force can be effectively reduced.

5.3 Impact of reduction ratio on unit normal pressure and rolling force

As shown in Fig. 5, the unit normal pressure increases with the increase of the reduction ratio, and it gets the maximum at the neutral point. The higher the reduction ratio, the value of neutral point increases slightly, and the arc length of deformation zone also increases obviously. As shown in Fig. 6, as the reduction ratio increases gradually, the rolling force becomes

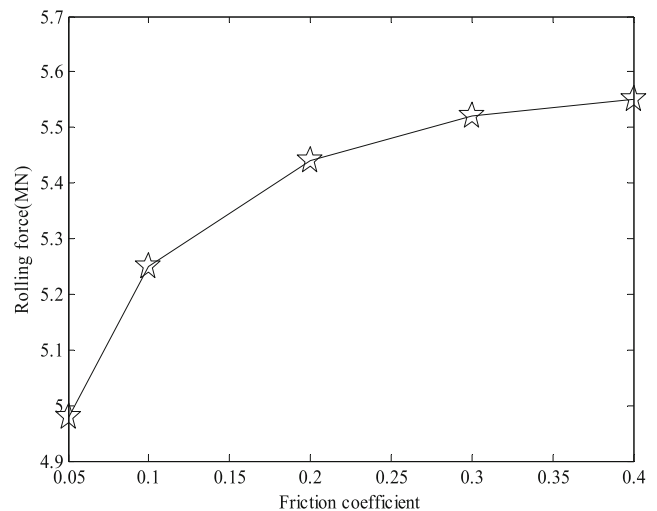


Fig. 4 Changes of rolling force with friction coefficient

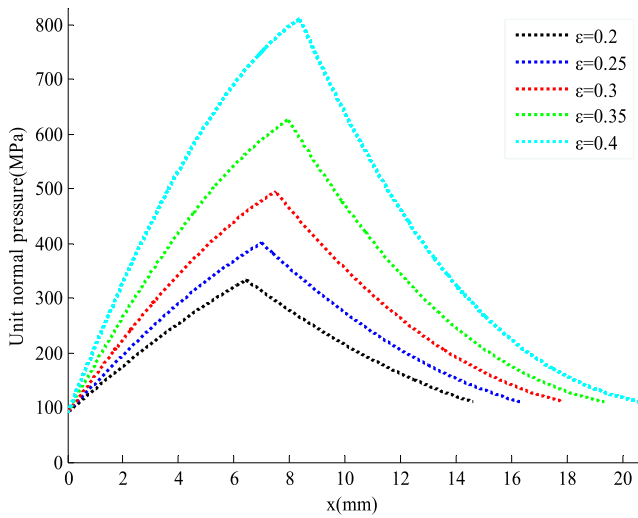


Fig. 5 Changes of unit normal pressure with reduction ratio

greater and greater. As the reduction ratio increases, the increase range of both unit normal pressure and rolling force becomes increasingly bigger.

5.4 Impact of shear strength on unit normal pressure and rolling force

The variation range of shear strength is from 40 to 90 MPa. As shown in Fig. 7, the unit normal pressure increases with the increase of the shear strength, and it reaches a peak at the neutral point. As shown in Fig. 8, with the growth of shear strength, the rolling force becomes increasingly bigger. Both the unit normal pressure and the rolling force almost linearly increase with the growth of shear strength.

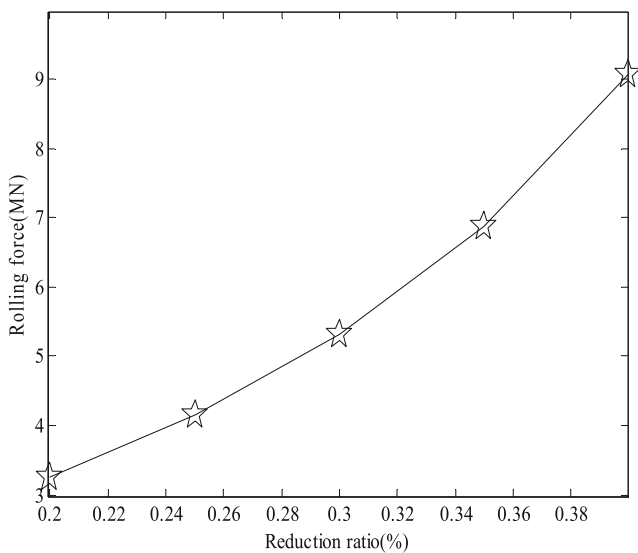


Fig. 6 Changes of rolling force with reduction ratio

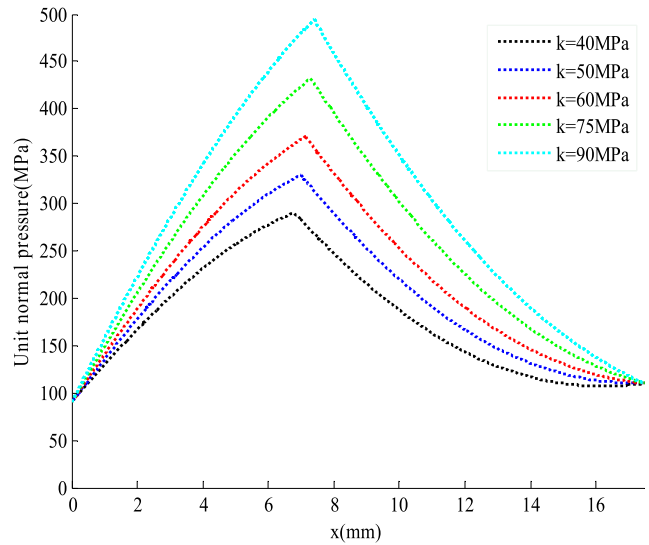


Fig. 7 Changes of unit normal pressure with shear strength

5.5 Impact of work roll flattening on unit normal pressure and rolling force

Considering the roll flattening effect, the most common formula of roll flattening is

$$R' = \left(1 + \frac{C_0 P}{\Delta h \cdot B} \right) \times R \tag{34}$$

where the roll flattening coefficient is: $C_0 = \frac{16(1-\nu_r^2)}{\pi \cdot E}$.

It can be seen from Fig. 9 that there is no obvious change of the unit normal pressure in the front-slip zone. Both the unit normal pressure in the backward slip area and its peak value increase slightly. The value of the neutral point and the arc length of the deformation area also increase slightly.

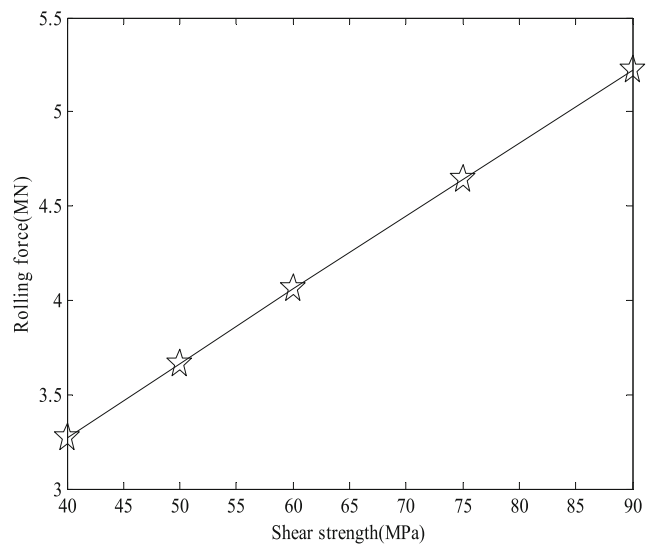


Fig. 8 Changes of rolling force with shear strength

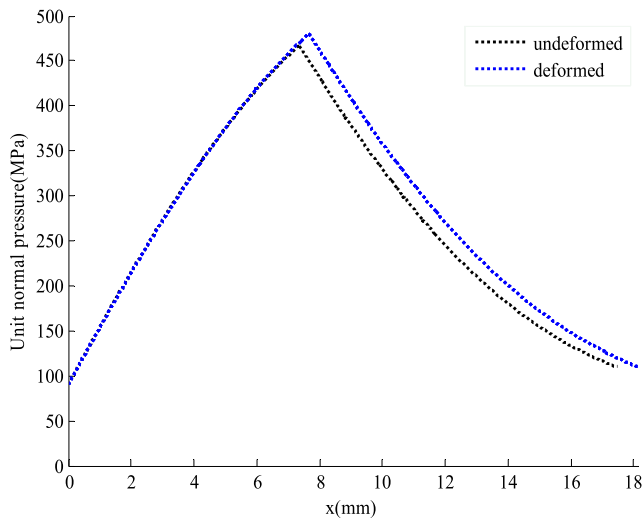


Fig. 9 Distribution of unit normal pressure with and without the roll flattening

It is necessary to iterate repeatedly between the rolling force expression and the roll flattening formula so as to realize the decoupling. In this simulation example, each iteration corresponds to a rolling pass. The condition of iterative termination is that the deviation of the rolling force of two adjacent times is less than 0.1%. As shown in Fig. 10, the raw data of the rolling force is 3723.877 kN, and the iteration converges at the fifth time, the rolling force after convergence is 3858.860 kN. This shows that roll flattening will cause an increase in the length of each micro-units and increase the rolling force.

6 Conclusion

1. The linearized unit pressure differential equation was obtained, based on Karman differential equation of unit pressure

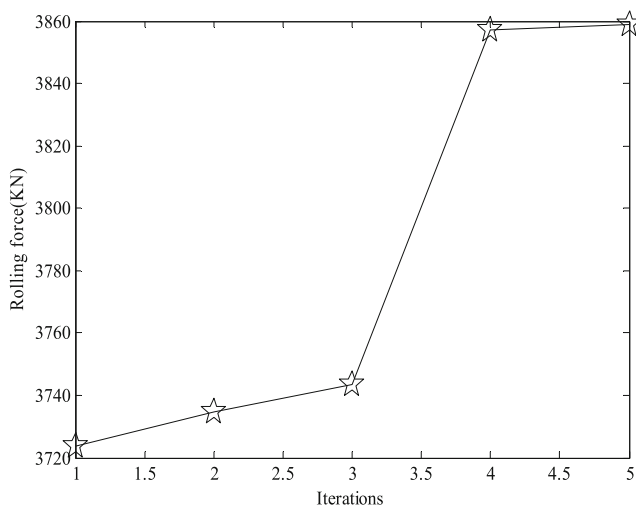


Fig. 10 Changes of rolling force in iteration

and Celikoff equation. The surface real contact area ratio was given by considering the probability density function and the root-mean-square roughness. According to the oil film thickness expression, rolling speed expression, friction law, and other conditions, it further acquired the expressions of total friction stress under mixed lubrication state of integrated boundary lubrication friction and hydrodynamic lubrication friction. Normally, the rolling lubrication state could not be achieved on pure dry friction or hydrodynamic lubrication, but on the mixed lubricant friction state of the coexistence of these two states. The total friction stress was applicable to the whole deformation zone and the general rolling mixed lubrication friction regime.

2. The expressions of unit normal pressure of the front-slip zone and the backward slip zone were obtained, based on the unit pressure differential equation after linearization and the total friction stress expression, and combining with the boundary conditions at the entrance and exit cross sections of the deformation zone. The dynamic rolling force model of cold rolling strip was established by numerical integral calculation. It is characterized by the consideration of the mixed lubrication friction state of the coexistence of boundary lubrication and hydrodynamic lubrication; therefore, this dynamic rolling force model is more universal, the prediction accuracy is higher, and it is closer to the actual industrial production.
3. The effects of friction coefficient, reduction ratio, shear strength, and roll flattening on the unit normal pressure along contact arc and the rolling force were analyzed in this paper. The simulation results showed that both the unit normal pressure and the rolling force increased with the increase of friction coefficient. But when the friction coefficient exceeded a certain value, the growth in unit normal pressure, and rolling force had slowed down. As the reduction ratio increased, the unit normal pressure and the rolling force were also gradually increasing, and the increase of their range was also getting bigger. The unit normal pressure and the rolling force almost increased linearly with the increase of shear strength. The unit normal pressure in the backward slip area and rolling force increased slightly with the roll flattening.
4. The verification of actual industrial production data showed that the prediction model of rolling force had high precision. It could be applied to the prediction of rolling force in cold rolling strip production and provide guidance for calibration of rolling mill equipment and parameter optimization of production technology.

Acknowledgements This work was supported by National Natural Science Foundation of China (Grant No. 61873227), Hundred Outstanding Innovative Talents Support Program of Hebei Province (Grant No.SLRC2019040), the China Postdoctoral Science Foundation funded project (Grant No. 2017 M620096), the Natural Science Foundation of Hebei Province, China (Grant No. E2017203144), and

the Special Program of Postdoctoral Foundation of Hebei Province (Grant No. B2017005007).

References

- Weisz-patrault D, Ehrlacher A, Legrand N (2013) Analytical inverse solution for coupled thermoelastic problem for the evaluation of contact stress during steel strip rolling. *Appl Math Model* 37(4): 2212–2229
- Qwamizadeh M, Kadkhodaei M, Salimi M (2014) Asymmetrical rolling analysis of bonded two-layer sheets and evaluation of outgoing curvature. *Int J Adv Manuf Tech* 73(1–4):521–533
- Yadav V, Singh AK, Dixit US (2015) Inverse estimation of thermal parameters and friction coefficient during warm flat rolling process. *Int J Mech Sci* 96–97:182–198
- Dixit US, Chandra S (2003) A neural network based methodology for the prediction of roll force and roll torque in fuzzy form for cold flat rolling process. *Int J Adv Manuf Tech* 22(11–12):883–889
- Weidlich F, Braga APV, da Silva Lima LGDB, Júnior MB, Souza RM (2019) The influence of rolling mill process parameters on roll thermal fatigue. *Int J Adv Manuf Tech*
- Linghu K, Jiang Z, Zhao J, Li F, Wei DB, Xu JZ, Zhang XM, Zhao XM (2014) 3D FEM analysis of strip shape during multi-pass rolling in a 6-high CVC cold rolling mill. *Int J Adv Manuf Tech* 74(9–12):1733–1745
- Li WG, Liu C, Liu B, Yan BK, Liu XH (2017) Modeling friction coefficient for roll force calculation during hot strip rolling. *Int J Adv Manuf Tech*
- Sun J, Liu YM, Wang QL, Hu YK, Zhang DH (2018) Mathematical model of lever arm coefficient in cold rolling process. *Int J Adv Manuf Tech* 97:1847–1859
- Poursina M, Rahmatipour M, Mirmohamadi H (2015) A new method for prediction of forward slip in the tandem cold rolling mill. *Int J Adv Manuf Tech* 78(9–12):1827–1835
- Lambiase F (2013) Optimization of shape rolling sequences by integrated artificial intelligent techniques. *Int J Adv Manuf Tech* 68(1–4):443–452
- Peck MC, Rough SL, Wilson DI (2005) Roller extrusion of a ceramic paste. *Ind Eng Chem Res* 44(11):4099–4111
- Sun J, Liu YM, Hu YK, Wang QL, Zhang DH, Zhao DW (2012) Application of hyperbolic sine velocity field for the analysis of tandem cold rolling. *Int J Mech Sci* 108–109:166–173
- Mancini E, Campana F, Sasso M, Newaz G (2012) Effects of cold rolling process variables on final surface quality of stainless steel thin strip. *Int J Adv Manuf Tech* 61(1–4):63–72
- Li YL, Cao JG, Kong N, Wen D, Ma HH, Zhou YS (2017) The effects of lubrication on profile and flatness control during ASR hot strip rolling. *Int J Adv Manuf Tech*
- Xie HB, Manabe KI, Furushima T, Tada K, Jiang ZY (2016) Lubrication characterisation analysis of stainless steel foil during micro rolling. *Int J Adv Manuf Tech* 82(1–4):65–73
- Wang QY (2004) Study on system dynamics of rolling mill in unsteady lubrication process. Central South University, 55–74. (in Chinese)
- Lo SW, Yang TC, Lin HS (2013) The lubricity of oil-in-water emulsion in cold strip rolling process under mixed lubrication. *Tribol Int* 66:125–133
- Brando JA, Meheux M, Ville F, Seabra JHO, Castro J (2012) Comparative overview of five gear oils in mixed and boundary film lubrication. *Tribol Int* 47(none):50–61
- Vadiraj A, Kamaraj M, Sreenivasan VS (2011) Wear and friction behavior of alloyed gray cast iron with solid lubricants under boundary lubrication. *Tribol Int* 44(10):1168–1173
- Ma CB, Zhu H (2011) An optimum design model for textured surface with elliptical-shape dimples under hydrodynamic lubrication. *Tribol Int* 44(9):987–995
- Liu LM, Zang Y, Chen YY (2011) Hydrodynamic analysis of partial film lubrication in the cold rolling process. *Int J Adv Manuf Tech* 54(5–8):489–493
- Hallberg H (2013) Influence of process parameters on grain refinement in AA1050 aluminum during cold rolling. *Int J Mech Sci* 66(2):260–272
- Bambach M, Häck A-S, Herty M (2017) Modeling steel rolling processes by fluid-like differential equations. *Appl Math Model* 43:155–169
- Lin JC (2002) Prediction of rolling force and deformation in three-dimensional cold rolling by using the finite-element method and a neural network. *Int J Adv Manuf Tech* 20(11):799–806
- Wu CH, Zhang LC, Pi Q, Li SQ, Jiang ZL (2018) A multi-field analysis of hydrodynamic lubrication in high speed rolling of metal strips. *Int J Mech Sci* S0020740318300067
- Alexandrov S, Mustafa Y, Lyamina E (2016) Steady planar ideal flow of anisotropic materials. *Meccanica* 51(9):2235–2241
- Stratmann A, Jacobs G, Hsu CJ, Gachot C, Burghardt G (2017) Antiwear tribofilm growth in rolling bearings under boundary lubrication conditions. *Tribol Int* 113
- Cao JZ, Liu YM, Luan FJ, Zhao DW (2016) The calculation of vertical rolling force by using angular bisector yield criterion and Pavlov principle. *Int J Adv Manuf Tech* 86(9–12):2701–2710
- Chen SX, Li WG, Liu XH (2014) Calculation of rolling pressure distribution and force based on improved Karman equation for hot strip mill. *Int J Mech Sci* 89:256–263
- Wu CH, Zhang LC, Li SQ, Jiang ZL, Qu PL (2014) A novel multi-scale statistical characterization of interface pressure and friction in metal strip rolling. *Int J Mech Sci* 89:391–402
- Zhang SH, Song BN, Wang XN, Zhao DW (2014) Analysis of plate rolling by MY criterion and global weighted velocity field. *Appl Math Model* 38(14):3485–3494
- Sun YK (2010) *Model and Control of Cold Hot Strip Mill* [M]. Beijing: Metallurgical Industry Press, pp 49–82 (in Chinese)
- Zhang X (2006) *Rolling theory* [M]. Metallurgical Industry Press, Beijing, pp 172–178 (in Chinese)
- Christensen H (1969) Stochastic models for hydrodynamic lubrication of rough surfaces. *Proc ImechE* 184(1969):1013–1026
- Jiang JH (2017) Study on stability and control of mill roll system based on nonlinear constraint of rolling force and friction force [D]. Yanshan University, pp 9–10 (in Chinese)

Publisher's note Springer Nature remains neutral with regard to jurisdictional claims in published maps and institutional affiliations.